

NetMoST: A network-based machine learning approach for subtyping schizophrenia using polygenic haplotype biomarkers

Xinru Wei^{1,2}, Shuai Dong², Zhao Su², Lili Tang^{1,5}, Pengfei Zhao^{1,5}, Chunyu Pan³, Fei Wang^{1,5*}, Yanqing Tang^{6,7,8*}, Weixiong Zhang^{4*}, Xizhe Zhang^{2*}

1. Early Intervention Unit, Department of Psychiatry, The Affiliated Brain Hospital of Nanjing Medical University, Nanjing, Jiangsu 210029, China;
2. School of Biomedical Engineering and Informatics, Nanjing Medical University, Nanjing, Jiangsu 210001, China
3. School of Computer Science and Engineering, Northeastern University, Shenyang, China
4. Department of Health Technology and Informatics, Department of Computing, The Hong Kong Polytechnic University, Hong Kong, China
5. Functional Brain Imaging Institute of Nanjing Medical University, Nanjing, China
6. Department of Psychiatry, The First Affiliated Hospital of China Medical University, Shenyang, China
7. Brain Function Research Section, The First Affiliated Hospital of China Medical University, Shenyang, China
8. Department of Gerontology, The First Affiliated Hospital of China Medical University, Shenyang, China

*: Correspondence: FW: fei.wang@yale.edu, YT: yanqingtang@163.com, WZ: weixiong.zhang@polyu.edu.hk, XZ: zhangxizhe@njmu.edu.cn

Abstract

Subtyping neuropsychiatric disorders like schizophrenia remains one of the most important albeit challenging themes for improving the diagnosis and treatment efficacy of complex diseases. At the root of the difficulty of this problem are the polygenicity and genetic heterogeneity of schizophrenia that render the standard diagnosis based on behavioral and cognitive indicators notoriously inaccurate. We developed a novel network-based machine-learning approach, netMoST, to subtyping psychiatric disorders. NetMoST identifies modules of polygenic haplotype biomarkers (PHBs) from genome-wide genotyping data as features for disease subtyping. We applied netMoST to subtype a cohort of schizophrenia subjects (n = 141) into three distinct biotypes with differentiable genetic and functional characteristics. The PHBs of the first biotype (28.4% of all patients) were enriched for neuroimmune functions, the PHBs of the second biotype (36.9%) were related to neurodevelopment and decreased cognitive measures, and the PHBs of the third biotype (34.7%) were associated with the transport of calcium ions and neurotransmitters. Neuroimaging patterns provided further support for these findings, with unique regional homogeneity (ReHo) patterns observed in the brains of each biotype compared with HCs, and statistically significant differences in ReHo observed between the biotypes. Our findings demonstrate the ability of netMoST to uncover novel biotypes in complex diseases such as schizophrenia via the analysis of genotyping data. The results also showed the power of exploring polygenic allelic patterns that transcend the conventional GWAS approaches.

INTRODUCTION

Schizophrenia (SCZ) is a devastating neuropsychiatric disorder with considerable morbidity and mortality¹⁻³ and exerts substantial health and socioeconomic burdens⁴. SCZ has a strong genetic predisposition and heritability estimated at 60-80%^{5, 6}. It is characterized by considerable etiological, pathophysiological, and symptom heterogeneity. SCZ shares genetic and clinical characteristics with other psychiatric disorders, such as bipolar disorder (BD) and major depressive disorder (MDD)⁷⁻⁹. However, current diagnostic criteria for SCZ are primarily based on behavioral and cognitive indicators¹⁰⁻¹², which are often difficult to quantify, inconsistent, and subjective. As a result, current diagnostic criteria often result in poorly informed therapeutic strategies, unpredictable treatment outcomes, and frequent relapses.

SCZ is a complex and heterogeneous disorder characterized by behavioral and cognitive symptoms⁵. Accurate subtyping SCZ is crucial for improving diagnosis and treatment outcomes and gaining a deeper understanding of the underlying pathogenesis and pathophysiology of the disease. One common approach for subtyping SCZ is based on the presence or absence of symptom profiles. For example, Dickison et al.¹³ identified two subgroups of SCZ based on psychotic symptoms, a “deficit” subtype, and a “distress” subtype. Lim et al.¹⁴ discovered four homogeneous groups of individuals with SCZ with different severity of cognitive impairment. However, SCZ symptoms can fluctuate depending on the stage of the illness, the presence of comorbid conditions, or the effects of medication¹⁵. This instability can make it challenging to classify patients accurately into subtypes and make it difficult to track disease progression or treatment response. Moreover, symptom-based subtyping provides little information on the underlying disease mechanisms and may not be well-suited for translating into effective therapeutic strategies. Another approach to SCZ subtyping is based on objective neurobiological features, including MRI-based neuroanatomical measures^{16, 17}, functional magnetic resonance imaging (fMRI)¹⁸, and combinations of electrophysiology and cognition¹⁹. Despite extensive research, valid neurobiological subtypes of SCZ have been elusive. This is primarily because the number of subtypes and their underlying biological features vary across studies, even when utilizing the same neuroimaging features. For example, Chand et al.¹⁶ and Xiao et al.¹⁷ independently identified two and three distinct neuroanatomical SCZ subtypes using gray matter volume as a neurobiological marker.

Manifestation of psychiatric symptoms and intermediate phenotypes result from the interaction between genetic predispositions and environmental triggers. Therefore, genetic risk factors are more potent biomarkers for psychiatric disorders like SCZ that have strong inheritability. However, little has been done to leverage SCZ genetic heterogeneity, although SCZ is a polygenic disease. Luo et al.²⁰ used a peripheral epigenome-wide DNA methylation array to cluster 63 SCZ patients into two biotypes, with one subtype displaying prominent methylation abnormalities and being associated with dysregulated immune function. Another recent study²¹ applied a multi-view clustering algorithm to clinical and SNPs data, grouping SCZ subjects into three biotypes with differential cognitive measures and disease courses. While these methods used genotyping data, they did not identify subtype-specific genetic risk factors, which could serve as potential biomarkers for the disease.

Subtyping and identifying genetic biomarkers for complex diseases such as SCZ are difficult because the two are intertwined. The interdependence of these two problems makes it challenging to identify biomarkers for SCZ. First, discovering biomarkers for complex diseases typically requires intergroup comparisons, i.e., comparing diseased and healthy groups, to identify key characteristics. However, individuals with a complex disease are often genetically heterogeneous and may carry multiple distinct biomarkers. This genetic heterogeneity can impede our ability to identify statistically significant biomarkers from the entire samples, leading to inconsistent and non-reproducible results. Overcoming this challenge requires subtyping the subjects and identifying biomarkers for every subtype. On the other hand, disease subtyping involves partitioning samples into groups with homogenous members. The similarity between

group members depends on the selection of patient features. Therefore, it is necessary to find essential biomarkers as features to calculate similarity for subtyping. However, as discussed earlier, biomarker identification depends on accurate subtyping. Therefore, disease subtyping and biomarker identification are interrelated. To our best knowledge, no literature has discussed this issue, and no method has been developed for addressing this issue.

Another challenge in subtyping SCZ is its polygenic nature. Complex diseases, such as SCZ, are caused by the interactions or associations of multiple genetic factors. Genome-wide association studies (GWAS) can help identify individual candidate genetic risk factors. However, these studies have limited power in finding genetic risk factors for complex diseases^{22, 23}. GWAS methods are designed to look for individual risk factors, so they fail to identify groups of related genetic factors, each of which may have small effect sizes when examined in isolation²⁴. Several approaches, such as the polygenic risk score (PRS)²⁵, have been attempted to address these limitations by looking for combinations of genetic variants to increase statistical power. However, these methods are designed for evaluation rather than discovery. Therefore, "present PRSs typically explain only a small fraction of trait variance"²⁶.

Here, we propose a novel algorithm to address the challenge of subtyping and identifying polygenic biomarkers for complex diseases through an integrated approach that combines subtyping and biomarker discovery. Taking SCZ as a case study, we apply the proposed method to subtype SCZ into three biotypes. The new biotypes are validated utilizing multimodal data, including genetic variations, brain neuroimaging patterns, and clinical features. We identified subtype-specific polygenic risk factors to understand the pathogenetic and pathophysiological features of SCZ. A noteworthy finding is the identification of an SCZ subtype defined by modules of genomic alleles on immune genes in the major histocompatibility complex of the human genome, suggesting the involvement of immunity in the pathogenesis and pathophysiology of SCZ.

RESULTS

Identifying subtypes and polygenic haplotype biomarkers for complex disease

Many complex diseases, such as schizophrenia (SCZ), are polygenic, meaning that variations at multiple genomic loci rather than individual ones drive the onset of disease phenotypes and disease progression. Additionally, these diseases are genetically heterogeneous, meaning that the same symptoms in different patients may be attributed to various genetic factors, indicating the existence of multiple disease mechanisms. As a result, complex diseases like SCZ have numerous polygenic risk factors. Genetic heterogeneity and multiple disease mechanisms necessitate adequate subtyping of diseases for accurate diagnosis and effective treatment.

We developed a novel *network module-based method for subtyping* (netMoST) of complex diseases like SCZ (Figure 1). The algorithm first constructs an SNP-allele network based on the Custom Correlation Coefficient (CCC), a novel method designed to capture genetic heterogeneity by computing a multi-faceted collection of correlation measurements. Compared to Pearson's Correlation Coefficient (PCC), CCC can identify larger patterns with stronger inter-correlations²⁷. The algorithm then utilizes network community detection algorithms to identify polygenic modules of functionally related SNPs. Polygenic modules statistically significantly correlated to the disease are selected as features. An unsupervised clustering algorithm is then applied to subtype the disease into biologically homogeneous subgroups. Further evaluation of the subtypes is performed by analyzing their polygenic modules using the same method used in the subtyping process but on samples specific to each subtype instead of all samples.

The central challenge in netMoST is defining and identifying polygenic risk factors. We conceptualize polygenic risk factors as modules of highly correlated SNP alleles across the entire genome. Utilizing SNP alleles can address genetic heterogeneity^{27, 28}, and SNP-allele modules may capture long-range genomic

associations across different chromosomes. Moreover, SNP-allele modules are specific to and characteristic of SCZ subjects, enabling distinction between SCZ cases and healthy controls. We term these SNP-allele modules *polygenic haplotype biomarkers* (PHBs) and apply them to stratify disease cases into biotypes.

We formulated the problem of finding PHBs as a problem of identifying modules of highly correlated nodes in a network of SNP alleles. We split the problem into two. The first is constructing a network of nodes representing SNP alleles and edges representing correlations between pairs of SNP alleles. To quantify SNP-allele correlations, we used the custom correlation coefficient (CCC) method²⁷ because it was designed to measure correlations between SNP alleles. The second problem is the general problem of finding modules of highly correlated nodes in a network, which has been extensively studied²⁹. We used the Louvain network-module detection method³⁰ in the current implementation of netMoST.

NetMoST defines three biological subtypes of schizophrenia

Polygenic haplotype biomarkers define three biotypes of schizophrenia

We applied our novel NetMoST method to subtype schizophrenia and identify polygenic biomarkers. A total of 425 participants were recruited, including 141 SCZ patients and 284 healthy controls (HCs). We carried out standard quality control on the genetic variants dataset, including 696,235 SNPs possessed by 425 individuals (detail see Method). We removed the individuals and SNPs that did not pass quality control. Finally, the 404,078 SNPs possessed by 141 SCZ patients and 283 HCs were retained (Figure 2A). Based on these SNP alleles, a network of SNP-alleles was constructed, consisting of 192,409 nodes (SNP alleles) and 480,339 interactions between SNP alleles. A total of 365,766 SNP-allele modules were identified. To identify the polygenic risk modules, we selected 426 risk SNP-allele modules with Odds Ratios (ORs) and Risk ratios (RR) larger than 1.2 (Figure 2A). These risk modules included 8,248 (4.3%) SNP alleles, which will be taken as the features for subtyping schizophrenia. Notably, these features consisted of more than one SNP allele, with an average of 19.4 alleles and a maximum of 150 alleles. The ORs of these features ranged from 1.23 to 8.22, with an average of 1.78 (Figure 2B, Supplemental File 1). Interestingly, it was observed that when analyzed individually, the SNPs within these modules had relatively low OR values, with a distribution around 1, indicating that they may not have a significant impact on the disease individually (Figure 2B). However, through our community detection algorithm, the OR values of these modules were significantly increased, suggesting that schizophrenia is a complex polygenic disorder and that identifying its genetic features requires an examination of multiple genes.

Furthermore, based on the 426 risk SNP-allele modules, we used Principle Component Analysis (PCA) and KMeans clustering algorithm to delineate three clusters or subtypes in the SCZ participants ($n = 141$). Biotype 1 consisted of 28.4% ($n = 40$) of the SCZ participants, biotype 2 consisted of 36.9% ($n = 52$), and biotype 3 consisted of 34.7% ($n = 49$) (Figure 2C). Demographic and clinical details of the subtypes are in Supplementary Table S1-S2. We applied the same network construction and module detection methods for each subtype to discover subtype-specific risk SNP-allele modules using more stringent criteria: $OR \geq 1.5$, a lower limit of 1.1 for 95% CI, and Yates's Correction p -value < 0.05 . We took subtype-specific risk SNP-allele modules as PHBs of SCZ. We found 83 PHBs for biotype 1, 264 PHBs for biotype 2, and 144 PHBs for biotype 3. Notably, the ORs of PHBs of the three biotypes were significantly greater than before subtyping (Figure 2D), showing that subtyping SCZ can enhance the ability to detect genetic risks of SCZ. Among three biotypes, biotype 2 had a smaller p value (biotype 1: $2.27E-31$, biotype 2: $3.55E-59$, biotype 3: $3.20E-41$) and a higher mean of OR (biotype 1: 2.84, biotype 2: 2.93, biotype 3: 2.73) in comparison with the OR distribution of PHBs obtained before subtyping, which indicated that it was more distinct from HCs than the other two biotypes.

To gain insight into the unique etiologies of the three biotypes of SCZ, we performed a gene function enrichment analysis (FUMAGWAS) on the host genes of the SNPs in these regions of PHBs or genes nearest

to them in the PHBs of each biotype (Figures 2E-2G). The SNPs in the biotype-2 PHBs were primarily associated with genes related to neurodevelopmental processes, including neurogenesis and neuron development and differentiation (Figure 2F). These biological pathways suggest that biotype 2 has significant genetic influences on neural systems, making it representative of the neurodevelopment of SCZ. In contrast, the biological functions of biotype 1 SNPs were significantly enriched with immune functions, including the regulation of immune processes, regulation of immune response, defense response, and innate immune response (Figure 2E). These findings highlight the relationship between immunity or inflammation and SCZ, suggesting that biotype 1 may be considered a highly inflammatory SCZ subgroup whose genetic variations lead to immune dysfunction and inflammation and subsequently contribute to the pathophysiology of SCZ. The biotype-3 SNPs were significantly enriched in the transport of calcium ions and neurotransmitters (Figure 2G), which are critical mediators of physiological functions in the central nervous system and have been implicated in the susceptibility or pathogenesis of psychiatric diseases. Some genetic risk factors of biotype 3 were also involved in glycoprotein biosynthetic processes, indicating that glycosylation plays an important role in SCZ. These results demonstrate that the three biotypes exhibit distinctive genetic patterns, reflecting a significant heterogeneity among the three biotypes of SCZ.

Subtype-specific polygenic haplotype biomarkers

To further assess the power of subtype-specific PHBs as biomarkers, we analyzed their overall effect sizes over SNPs chosen by the standard association analysis using the logistic regression model in PLINK v1.9³¹. Our results revealed that individuals in biotype 1 carried at least 49 (59%) of the 83 PHBs, with a mean of 61 PHBs for all SCZ subjects. Each patient in biotype 2 possessed at least 158 (60%) of the 246 PHBs. In biotype 3, each subject carried at least 99 (69%) of the 144 PHBs, with an average of 109 (76%) PHBs across all patients. These findings suggest that PHBs may serve as robust biomarkers for SCZ. Notably, approximately 31.5% of PHBs (biotype 1: 21.7%, biotype 2: 39.8%, and biotype 3: 22.2%) contained SNP loci spanning various chromosomes, with many of these loci located in noncoding or nongenic regions.

To characterize the PHBs as biotype signatures and appreciate their biological functions, we selected one PHB with a large odds ratio (OR) and a sufficient number of SNP alleles in genic regions from each subtype. We then analyzed the potential function of these PHBs using the functions of the host genes of the SNPs in the PHBs. The PHB for biotype 1 consisted of 71 SNP-alleles, surprisingly, distributed across nine chromosomes (Figure 3A). Interestingly, 25% of SCZ subjects in biotype 1 carried this PHB, compared to 6.2% of healthy controls, resulting in the highest OR of 5.04 (CI: 2.03-12.50) for biotype 1. Moreover, 43 (60.6%) of the SNP alleles of this PHB resided in the major histocompatibility complex (MHC) on chromosome 6, which is known to be critical to immunity³². Two SCZ-susceptible genes, HLA-DQA1 and HLA-DQB1^{33, 34}, are also located in this region (Figure 3A, eFigure 5A). Furthermore, we computed various centrality measures, including the degree centrality³⁵, average neighbor degree³⁶, closeness centrality³⁷, and pagerank^{38, 39} for every SNP allele in the PHB. These calculations revealed that SNP alleles in the MHC region had greater centrality, average neighbor degree, closeness centrality, and PageRank index, indicating their functional importance (eFigure 1). For comparison, we also calculated the OR for each SNP in this PHB using standard association analysis based logistic regression model in PLINK³¹. Fifteen (21.1% of the 71) SNPs were found to be statistically significant (p-value < 0.05, association analysis using the logistic regression model). The SNP with the highest OR (MHC:rs9268199 in gene C6orf10) was carried by 28.8% cases in biotype 1 but also by 12.2% of healthy controls, resulting in an OR of 2.96 (CI: 1.71- 5.11), which was significantly lower than the OR of 5.04 for the top-ranked PHB (Figure 3B).

It is noteworthy that the top 10 ranked PHBs of biotype 2 displayed significant odds ratios (ORs) ranging from 4.22 to 57.68 (Supplemental File 1). Many SNP loci in these PHBs were located non-coding or in non-genic regions. To characterize the potential functions of biotype 2, we selected a representative PHB,

whose 84.5% SNPs were in protein-coding genes, for further analysis. This PHB appeared in 30% of biotype-2 cases and 7.2% of HCs, resulting in an OR of 5.46 (CI: 2.56-11.65). It was composed of 71 SNP alleles from 11 genes (GRM5, NOTCH4, SORBS2, IL1RAPL1, STK19, TNXB, PPT2, RNF5, PBX2, TMEM132D, and FLRT2) spanning eight chromosomes (Figure 3C, eFigure 5B), representing a long-range haplotype over multiple genes across multiple chromosomes (eFigure 2). It is worth noting that the standard association analysis in Plink detected only one SNP (rs9994907, located in SORBS2) with statistical significance (OR: 1.56, p-value < 0.05, logistic regression analysis). The SNP-alleles of this PHB in NOTCH4 (Notch Receptor 4) on chromosome 6, GRM5 (Glutamate Metabotropic Receptor 5) on chromosome 11, and IL1RAPL1 (Interleukin 1 Receptor Accessory Protein Like 1) on chromosome X displayed significant network centralities, including average neighbor degrees, closeness centralities, and Pagerank values (eFigure 3). These three genes were involved in the development of SCZ. Specifically, fifteen SNP-alleles were on GRM5, which has been regarded as a promising target for treating cognitive deficits of SCZ⁴⁰. NOTCH4, which hosts eight SNP-alleles in this PHB, had been repeatedly reported to be strongly associated with SCZ⁴¹. IL1RAPL1 is located in a critical region on chromosome X associated with a non-syndromic form of X-linked intellectual disability⁴². IL1RAPL1 was expressed abundantly in post-natal brain structures involved in the hippocampal memory system, suggesting a specialized role in regulating physiological processes underlying memory and cognition abilities⁴². These results demonstrated that the genetic features captured by the PHB tended to be involved in developing and regulating neural systems, especially cognition.

Similarly, biotype 3 had a PHB with an OR of 12.39 (CI: 3.46-44.32). It appeared in 15.56% of biotype-3 subjects and 1.47% of HCs. This PHB comprised 67 SNP-alleles, most of which existed in three genes, CDKAL1, PTPRD, and CACNA2D1 (Figure 3E, eFigure 5C). Twenty-six SNP-alleles were located in CDKAL1, a gene that rendered people with SCZ genetically predisposed to type 2 diabetes⁴³, suggesting CDKAL1 may be a shared genetic risk factor for both diseases⁴⁴. The SNP-alleles in CDKAL1 had a greater centrality and average neighbor degree, highlighting their role in this PHB. Gene PTPRD contained eight SNP-alleles, which encoded a molecule for signal transduction. CACNA2D1 hosted four SNP-alleles, a gene encoding a voltage-gated calcium channel-related gene. The gene was critical for mediating intracellular Ca²⁺ influx and, therefore, responsible for signaling transmission across synapses⁴⁵. Similar to the other two biotypes, the SNPs selected by the single-marker method Plink had much lower ORs than that of the PHB (Figure 3F).

In summary, the three representative PHBs chosen by netMoST for the three biotypes had higher ORs than the single-SNP counterparts determined by standard association analysis using the logistic regression model in PLINK (Figures 3A-3F). The significance of this result is multifold. It showed that netMoST could capture the potential genetic risk ignored by conventional single-marker-based methods such as Plink. netMoST can identify combinatorial, polygenic risk factors that may span multiple chromosomes, which were large haplotypes with long-range linkage associations (Figures 3A, 3C and 3F).

Subtype-specific alterations of neuroimaging patterns

We found significant differential alterations in neuroimaging patterns among three biotypes when compared to healthy controls (HCs). Specifically, the regional homogeneity (ReHo) of the three biotypes was significantly elevated in the frontal lobe, whereas the brain regions displaying decreased ReHo were distinctive among the three biotypes. Biotype 1 had increased considerably ReHo in the frontal lobe (superior frontal gyrus, middle frontal gyrus, and medial frontal gyrus) but significantly decreased ReHo in the occipital lobe and lingual gyrus when compared to HCs (Figure 4A). Biotype 2 had significantly increased ReHo in the frontal lobe (inferior frontal gyrus, middle frontal gyrus, and orbital part of the inferior frontal gyrus) but significantly decreased ReHo in the occipital lobe, cuneus, and lingual gyrus when compared to HCs (Figure 4B). Biotype 3 was found to have significantly increased ReHo in the frontal lobe (superior frontal gyrus, medial of superior frontal gyrus, and orbital part of the inferior frontal gyrus) but significantly

decreased ReHo in the parietal lobe, postcentral gyrus, precentral gyrus, and temporal lobe when compared to HCs (Figure 4C). Additionally, significant differences in ReHo were observed among the three biotypes (Figures 4D-4E), with biotype 2 displaying significantly higher ReHo compared to biotype 1 in the inferior frontal gyrus and lower ReHo compared to biotype 3 in the inferior frontal gyrus. These distinct intermediate phenotypes of neuroimaging characteristics in ReHo among the three biotypes support the distinctive polygenic risk factors of these biotypes and illustrate the power of netMod-ST as a diagnostic tool.

Subtype-specific clinical characteristics

We used a one-way ANOVA analysis to compare the differences in behavioral symptoms assessed by Brief Psychiatric Rating Scale (BPRS). The BPRS consist of five-factor scores, and the three biotypes showed a significant difference in three of them, including Anxiety and Depression, Hostility-suspicion, and Disorganized Cognitive Processing (Figures 4F-4H). Overall, biotype 1 showed more severe behavioral symptoms in Hostility-suspicion and Disorganized Cognitive Processing. Specifically, biotype 1 had a higher factor score of Hostility-suspicion (P-value of 0.002 after LSD correction) compared with biotype 2 (Figure 4G) and Disorganized Cognitive Processing compared with the other two biotypes (P-value of 0.007 after LSD correction) (Figure 4H). Biotype 3 showed more severe Anxiety and Depression, as indicated by the lowest score of Anxiety and Depression (P-value of 0.04 after LSD correction) (Figure 4F).

Similarly, one-way ANOVA analysis was used to evaluate the difference in cognitive ability among three biotypes and healthy controls (HCs) by utilizing two cognitive function measures, the MATRICS Consensus Cognitive Battery (MCCB) and Wisconsin Card Sorting Test (WCST). The results revealed that the three biotypes exhibited varying levels of cognitive impairments compared to HCs, as evidenced by lower T-scores of MCCB and higher scores of non-perseverative errors (NPE) on the WCST (Figures 4I-4J). Specifically, biotype 2 was found to exhibit the worst cognitive performance, as indicated by the lowest T3 score of MCCB and the highest NPE score of WCST. Statistical analysis further revealed that the T3 score of MCCB in biotype 2 was significantly lower than the other two biotypes (P-values of 0.03 and 0.04 after LSD correction) (Figure 4I), and the NPE score of WCST was substantially higher than biotype 3 (P-value of 0.02 after LSD correction) (Figure 4J).

DISCUSSION

Most complex diseases have high genetic heterogeneity. Several GWAS studies have been previously conducted, and hundreds of individual SNPs associated with complex diseases have been identified⁶. However, identifying genetic risk factors for complex diseases has proven challenging, even in extremely large GWAS⁴⁶. These challenges are mainly attributed to the fact that diagnostic systems for most disease distinguish subtypes due to clinical phenomenology rather than physiological characteristics. Traditional GWAS also can not characterize the multi-genetic interaction effect on most complex diseases, such as SCZ, as we discussed earlier.

In this study, we proposed netMoST, a novel approach combining community detection and clustering, which could address the polygenesis and genetic heterogeneity of complex diseases. Briefly, our approach hinges upon two critical ideas. First, netMoST used CCC⁴⁷, a correlation metric specially designed for SNP-alleles, to construct an SNP-allele network, which could effectively characterize the potential interaction between genetic variations and combine inter-correlated genetic variations with a low computational cost for high-dimensional SNP alleles. And then, the Louvain community detection was used to extract SNP-allele modules or PHBs from specific SNP-allele networks of disease (Figure 1). Theoretically, the network analysis for extracting SNP-alleles modules could solve the polygenesis of complex diseases, including SCZ. As expected, the subtype-specific PHBs as one unit showed a higher odd ratio than any SNP in subtype-

specific PHB (Figures 3A-3F, Supplemental File 1). These results indicated that netMoST could combine and discriminate genetic risk and transcended single-marker methods. Second, Considering the heterogeneity of complex diseases, the clustering methods were performed to discover disease subtypes based on SNP-alleles modules. Then the PHBs of every subtype were identified by repeating the network-module method in netMoST. Compared with SCZ before subtyping, the ORs of the PHBs of each subtype were significantly elevated (Figure 2D), a result consistent with our hypothesis that reasonable classification of complex disease would enhance the ability to detect genetic risk and help capture the potential genetic pattern within subtypes. Note that gene set enrichment of PHBs for each subtype illuminate that the three biotypes have discriminative genetic patterns, including inflammation responses, nervous system development, and the transport of calcium ions and neurotransmitters (Figures 2E-2G). Meanwhile, the unique neuroimaging characteristics among the three biotypes also emphasize the existence of three subtypes with different PHBs of SCZ (Figures 4A-4E). Notably, compared with the other two biotypes, biotype 2 was the most distinct subtype of SCZ, representing significant cognitive function impairment (Figures 4I-4J).

It is worth noting that the genetic pattern of biotype 1 was primarily characterized by the involvement in immune/inflammatory regulation. Additionally, the PHB with the highest OR showed a high correlation with immunity, and most of its genetic variations of it were located in the MHC region, which has long been assumed to harbor genetic variants conferring the risk of SCZ⁴⁸. Network analysis also emphasized the importance of the MHC region in the subtype-specific PHB of biotype 1 (eFigure1). Consistent with the previous study, the findings that two key genes, HLA-DQA1, HLA-DQB1 corresponding to these alleles, are identified and further demonstrate the association of biotype 1 with the immune system. There exists more evidence for the involvement of immune proteins in the function of the CNS, such as differentiation and migration and synaptic plasticity^{49, 50}. These core biological processes are related to the pathogenesis of schizophrenia⁵¹. Furthermore, biotype 1 had significantly increased ReHo in the frontal lobe and significantly decreased in the occipital lobe and lingual gyrus, compared with HCs. Conceivably, immune-related genetic variations may involve inflammation response in biotype 1, affecting fundamental brain functions by compromising synaptic plasticity, neurogenesis and neuronal differentiation and migration.

Significantly different from biotype 1, biotype 2 is a typical subtype of SCZ with more severe cognitive impairment and showed a neurodevelopment-associated genetic pattern, whose genetic variations were involved in neuron development and differentiation as neurogenesis (Figure 2F). And the subtype-specific PHB of biotype 2 emerged as the interaction pattern between multi-genes across different chromosomes (Figure 3C, eFigure 5A2). The crucial genetic risk genes, including NOTCH4, GRM5, and IL1RAPL1, were identified through the network analysis, which has been reported in previous GWAS analyses. In particular, IL1RAPL1, encoding the interleukin 1 receptor, have been shown to play a specialized role in the physiological processes underlying memory and learning abilities. The NOTCH4 has been repeatedly reported that it could regulate differentiation and migration of neural stem cells and play a genetic risk to media neurodevelopment. Similarly, previous studies have emphasized the importance of synaptic plasticity in early brain development⁵², particularly glutamatergic neurotransmission⁵³. Indeed, this subtype may be caused by the interactions of genetic variations, representing neurodevelopmental abnormalities. Additionally, the ReHo of biotype 2 is significantly decreased in the frontal lobe and increased in the occipital lobe, Cuneus, and lingual gyrus compared to HCs.

Biotype 3 was enriched with transporters of calcium ions and neurotransmitters (Figure 2F). The biological processes related to them are essential to shaping neural circuits during development and for mature brain function⁵⁴. The core pathology of biotype 3 may be the impaired neuromodulation of synaptic signaling transmission, leading to abnormal functional integration of neural systems. Interestingly, besides the risk genes related to the transport of calcium ions and neurotransmitters, such as PTPRD and CACNA2D1, we identified CDKAL1, a gene susceptible to type 2 diabetes. The gene hosts 38.8% SNP alleles

in the subtype-specific PHB with the highest OR, indicating that CDKAL1 may be a shared genetic risk factor for both diseases. Additionally, biotype 3 has different neuroimaging features than the other two subtypes. ReHo was significantly increased in the frontal lobe and significantly decreased in the parietal lobe, postcentral gyrus, precentral gyrus, and temporal lobe compared to HCs.

Our research developed a novel netMoST approach for identifying biologically-based complex disease biotypes. It could be applied to any existing genomic DNA genotyping datasets of disease and effectively address the polygenicity and heterogeneity of the disease. We applied the netMoST approach to SCZ and identified three PHBs-based biotypes. Significantly, the three PHBs of SCZ exhibited unique genetic patterns, neuroimaging and cognitive impairment (Figures 4A-4I), which verified the feasibility and validity of our proposed approach capable of discovering underlying subtypes of complex disease.

Summary

In summary, we introduced netMoST approach, which combines community detection and clustering to identify module-based biotypes. We applied it to SCZ and extracted subtype-specific PHBs for each biotype. Three unique biotypes of SCZ were discovered, and they had different genetic patterns and neuroimage features, which provides deep insights into the neuropathogenesis of the SCZ biotypes and informs future translational clinical studies.

MATERIALS AND METHOD

Subjects and data collection and preprocessing

A cohort of 141 individuals diagnosed with schizophrenia (SCZ) was recruited from the Shenyang Mental Health Center and the First Affiliated Hospital of China Medical University in Shenyang, China. In addition, advertisements recruited 284 healthy controls (HCs) from local communities. Behavioral symptoms were assessed using the Brief Psychiatric Rating Scale (BPRS). Cognitive function was assessed using the Wisconsin Card Sorting Test (WCST) and MATRICS Consensus Cognitive Battery (MCCB). Demographic and clinical characteristics are detailed in Supplementary Table 1. Two professionally trained psychiatrists made the diagnoses based on the structured clinical interview for DSM-IV Axis I Disorders participants over 18 and the Schedule for Affective Disorders and Schizophrenia for School-Age Children-present and Lifetime Version (K-SADS-PL) for participants under 18 years old. All patients met DSM-IV criteria for SCZ and had no other comorbid Axis I disorders. The healthy controls did not have a personal history of psychotic or recurrent mood disorders. Exclusion criteria for the study included: (1) the presence of organic brain disease; (2) a history of substance abuse or dependence (excluding tobacco); (3) a previous history of head injury, epilepsy, or coma; (4) contraindications for magnetic resonance examination. The Institutional Review Board of China Medical University approved the study, and informed consent was obtained from all participants.

Genotyping and Quality Control

Peripheral venous blood samples (5 mL) were collected from each subject using EDTA Vacutainer tubes and centrifuged at 2000 rpm for 10 min. Subsequently, plasma and blood cells were separated and stored at -80°C for genomic (100 µL each) analyses. All participants were genotyped using whole blood and the Illumina Global Screening Array-24 v1.0 BeadChip, which covers 642,824 fixed genetic variants and 53,411 customized variants specific to Han Chinese populations. The assays were performed following the manufacturer's recommendations, and Plink v1.9³¹ was employed for quality control of the genotyping data. Single Nucleotide Polymorphisms (SNPs) with a minor allele frequency (MAF) less than 1%, call rate less than 95% or Hardy-Weinberg equilibrium (HWE) p-value less than 10⁻⁵ were excluded. Individuals with excessive missingness greater than 5% were removed. The final genotyping data included 404,078 genetic

variants for 424 participants.

Functional MRI Acquisition and Preprocessing

Magnetic Resonance Imaging (MRI) scans were obtained using a GE Signa HD 3.0T scanner with a standard 8-channel head coil at the First Affiliated Hospital of China Medical University in Shenyang, China. The functional images were acquired using a spin echo planar imaging (EPI) sequence, with the following parameters: repetition time (RT) = 2,000 ms, echo time (TE) = 30 ms, flip angle = 90°, the field of view = 240×240 mm², matrix = 64 x 64. A total of 35 axial slices were collected with 3 mm thicknesses without a gap.

The Functional MRI (fMRI) preprocessing was performed using the Statistical Parametric Mapping 8 (SPM8; <http://www.fil.ion.ucl.ac.uk/spm>) and the Data Processing Assistant for R-functional MRI (DPARSF; <http://www.restfmri.net/forum/DPARSF>)^{6, 55}. The first 10 time points of functional images were discarded to ensure magnetization stabilization, followed by slice timing correction, motion correction, and spatial normalization. The images were then normalized to Montreal Neurological Institute (MNI) space using a standard EPI template with a re-sampling voxel volume of 3 mm x 3 mm x 3 mm. The images were then spatially smoothed with a 6 mm full-width-at-half-maximum (FWHM) Gaussian kernel. To minimize the effects of frequency drifts and high-frequency noise, all-time courses were filtered between 0.01–0.08 Hz. After preprocessing, we applied DPARSF to calculate Regional Homogeneity (ReHo), which was used to measure the similarity of the time series of a given voxel to those of its adjacent 26 voxels. The whole brain average normalized the ReHo values.

Identifying disease subtypes based on polygenetic modules

Custom Correlation Coefficient (CCC)⁴⁷ was adopted to construct an SNP-allelic network for a given GWAS dataset. In an allelic network, an SNP is represented by two nodes, one for each SNP allele. An edge is introduced to link two alleles of different SNPs if their correlation is above a significance threshold. In our current implementation, we used a stringent CCC threshold of 0.68 to construct the SNP-allele network using data of all participants for subtyping. Louvain community detection algorithm³⁰ was applied to identify SNP-allele modules from an allelic network with tight connections within a module and relatively sparse connections across modules. It is a multi-phase, iterative heuristic community detection algorithm for optimizing the Q-function of global modularity, which describes the tightness of the modules or communities^{30, 56}. Compared with other community methods, Louvain can extract modules in large networks using less computation.

To identify the genetic features of SCZ, we computed the frequencies, odds ratio (OR), and risk ratios (RR) for every module in SCZ cases and HCs. The OR was computed as $OR = ad/bc$, where a and b equal the numbers of the module possessed by the SCZ cases and HCs, respectively. Each subject has two allelic combinations that include the SNPs in the bloc. The sum of the combinations that are not identical to the module is represented by c for the SCZ cases and d for the HCs. The RR was computed as $RR = a(b+d)/b(a+c)$. The 95% confidence interval (CI) was defined as $e^{[ln(OR) \pm 1.96sqrt(1/a+1/b+1/c+1/d)]}$, where ln is the natural log and $sqrt$ is the square root. We selected those SNP-allele modules with $OR \geq 1.2$ and frequency ratio ≥ 1.2 as risk SNP-allele modules for subtyping SCZ. The 426 risk SNP-allele modules were taken as features to define the biotypes of SCZ. We combined Principal Component Analysis (PCA)⁵⁷ and miniBatchKmeans⁵⁸ to cluster the SCZ cases into three groups or subtypes.

Identify subtype-specific polygenic haplotype biomarkers

We used a more stringent CCC threshold of 0.72 to build an SNP-allele network for each biotype to identify subtype-specific polygenic haplotype biomarkers (PHBs). These two networks had similar network densities, where the average node degree in the two networks was 2~2.5.

Permutation trials for avoiding false-positive edges

To avoid false-positive edges in an allele-specific network, we randomly shuffled the genotypes of the individuals with the original allele and genotype frequency of every SNP intact. After each randomization, we recalculated the CCC value for every pair of SNP alleles, we would filter out the false-positive edge if the CCC value for one pair of SNP alleles was lower than the criterion threshold in the original network after multiple permutations.

Permutation trials

To discover subtype-specific PHBs, we randomly permuted the phenotype labels across the subtype of SCZ and 283 HCs. We then computed the G-test score for every module for these randomized groups of individuals and repeated these trials 1,000 times. We retained the modules with statistical significance p-values of G-test scores below a threshold and discarded the modules that failed the permutation test.

Bootstrapping trials

We randomly selected eighty percent of the cases and eighty percent of the HCs, computed the ORs for the modules of every subtype, and repeated these trials 1,000 times. We calculated the OR and p-value for every module in each trial. We computed the mean OR and average 95% confidence intervals over the 1,000 trials for every module in each subtype. We remove the modules with ORs < 1.5 or 95% confidence interval ≤ 1.05 over the 1,000 random samplings.

To improve the diagnostic power, we looked for subtype-specific PHBs. It was done the same way as finding modules for SCZ, but instead of using all the SCZ cases, only the SCZ cases belonging to each subtype were used to construct a new, subtype-specific SNP-allele network. Meanwhile, we used more stringent criteria to select subtype-specific PHBs: OR ≥ 1.5 , a lower limit of 95% CI ≥ 1.1 , and Yates's correction p-value < 0.05 . Additionally, all the subtype-specific PHBs underwent permutation and bootstrapping trials. Specifically, from the PHBs sorted by ORs (Supplemental Table1), we selected the subtype-specific PHB with the highest OR and calculated the degree centrality³⁵, average neighbor degree³⁶, closeness centrality³⁷ and pagerank^{38, 39} for the PHB topology network to characterize every SNP-allele belonging to the PHB.

Subtype validation across multi-modal biological data

To assess the diagnostic capability of PHB-based subtyping, we identified the PHBs of SCZ from 426 risk SNP-alleles modules following the stringent criteria of subtype-specific PHBs. We used the average OR as the evaluation metric to compare PHBs before and after subtyping. The differences between PHBs before and after subtyping were analyzed by one-way ANOVA.

Gene function enrichment analysis

A gene set enrichment analysis was performed on the genes hosting the SNPs in a PHB or genes closest to the SNPs using FUMAGWAS⁵⁹. For SNPs in noncoding transcript, we extended the boundaries of the genic coordinates upstream 15kb and downstream 10kb to capture the adjacent risk genes. The enrichment analysis utilized molecular pathways from the biological processes of gene ontology (GO)⁶⁰. Biological Processes (BP) with FDR-corrected p-value < 0.05 were taken as significantly enriched.

Comparison of ReHo alterations between subtypes and HC

To identify regional homogeneity (ReHo) alteration in fMRI for subtypes and HC, we used DPABI⁶¹ to perform the two sample t-tests for comparing the ReHo values between subtypes and each subtype with HC. For the two-sample t-tests, gender and age were included as covariates. The statistical significance level was set at p-values < 0.05 using the Gaussian random field (GRF) correction.

Comparison of clinical and cognitive characteristics of subtypes

One-way ANOVA analysis was performed on a patient group to determine significant differences in cognitive ability measured by the Wisconsin Card Sorting Test (WCST) and MATRICS Consensus Cognitive Battery (MCCB), as well as behavioral symptoms assessed by Brief Psychiatric Rating Scale (BPRS) between subtypes of SCZ cases and HCs. The statistical significance level was set at p-values < 0.05 after the Least Significant Difference (LSD) correction.

Brief Psychiatric Rating Scale (BPRS) factor scores were identified from the exploratory factor analysis (EFA) using the principal component factor method, which results in a parsimonious list of factors using BPRS items. Five interpretable and clinically relevant factors were identified: anxiety and Depression, Negative symptoms, Hostility-suspicion, activation, and Disorganized Cognitive Processing.

The WCST and MCCB are routine neurocognitive tasks frequently used to assess cognitive flexibility in patients with mental disorders, especially SCZ. WCST consists of 128 response cards and four stimulus cards. The geometric shapes on the cards are different in color (red, green, blue, or yellow), form (circles, stars, squares, or crosses), and number (1, 2, 3, 4). During the test, the subjects were expected to accurately sort every response card with one of four stimulus cards by the feedback (right or wrong) given to them based on a sorting rule. Five WCST performance measures were used to assess cognitive abilities: the numbers of categories completed (CC), correct responses (CR), total errors (TE), perseverative errors (PE, i.e., the subject persisted in making an incorrect sorting choice), and non-perseverative errors (NPE, i.e., incorrect responses other than PE). Higher scores of CC and CR indicated good cognitive performance, while higher scores of TE, PE, and NPE suggested poor cognitive function. MCCB includes seven psychological dimensions and ten subtests⁵⁰. All test scores were converted to T-scores (T1-T10, mean 50, standard deviation 10) based on original scores. A higher T-score for MCCB indicates good cognitive function.

Competing interests

The authors declare that they have no competing interests

Funding

This work was supported in part by the National Natural Science Foundation of China (grant 62176129), National Key Research and Development Program (2022YFC2405603), the United States National Institutes of Health (grant R01-GM100364), the Hong Kong Global STEM Professorship Scheme, National Science Fund for Distinguished Young Scholars (81725005), NSFC-Guangdong Joint Fund (U20A6005), the National Key R&D Program of China (2018YFC1311600 and 2016YFC1306900) and Liaoning Revitalization Talents Program (XLYC1808036). The work was partly supported by the Hong Kong Global STEM Professor Scheme and the Hong Kong Jockey Club Charities Trust.

Authors' contributions

Xizhe Zhang, Fei Wang, and Weixiong Zhang conceived and designed the research. Xinru Wei implemented the algorithm, collected and analyzed the data, and helped with writing the manuscript and preparing the figures. Lili Tang, Zhao Su, Pengfei Zhao helped with preparing the figures. Yanqing Tang, Shuai Dong, Chunyu Pan collected the data. Xizhe Zhang and Weixiong Zhang analyzed the data and drafted the manuscript.

REFERENCE

1. McCutcheon, R.A., Marques, T.R. & Howes, O.D. Schizophrenia—an overview. *JAMA psychiatry* **77**, 201-210 (2020).
2. McGrath, J., Saha, S., Chant, D. & Welham, J. Schizophrenia: A Concise Overview of Incidence, Prevalence, and Mortality. *Epidemiologic Reviews* **30**, 67-76 (2008).
3. Hjorthøj, C., Stürup, A.E., McGrath, J.J. & Nordentoft, M. Years of potential life lost and life expectancy in

- schizophrenia: a systematic review and meta-analysis. *The Lancet Psychiatry* **4**, 295-301 (2017).
4. Kadakia, A. et al. The Economic Burden of Schizophrenia in the United States. *The Journal of Clinical Psychiatry* **83**, 43278 (2022).
 5. Owen, M.J., Sawa, A. & Mortensen, P.B. Schizophrenia. *Lancet* **388**, 86-97 (2016).
 6. Biological insights from 108 schizophrenia-associated genetic loci. *Nature* **511**, 421-427 (2014).
 7. Consortium, C.-D.G.o.t.P.G. Identification of risk loci with shared effects on five major psychiatric disorders: a genome-wide analysis. *The Lancet* **381**, 1371-1379 (2013).
 8. Goodkind, M. et al. Identification of a common neurobiological substrate for mental illness. *JAMA psychiatry* **72**, 305-315 (2015).
 9. Fortgang, R.G., Hultman, C.M., van Erp, T.G. & Cannon, T.D. Multidimensional assessment of impulsivity in schizophrenia, bipolar disorder, and major depressive disorder: testing for shared endophenotypes. *Psychological medicine* **46**, 1497-1507 (2016).
 10. Cheniaux, E., Landeira-Fernandez, J. & Versiani, M. The diagnoses of schizophrenia, schizoaffective disorder, bipolar disorder and unipolar depression: interrater reliability and congruence between DSM-IV and ICD-10. *Psychopathology* **42**, 293-298 (2009).
 11. Tandon, R. et al. Definition and description of schizophrenia in the DSM-5. *Schizophrenia research* **150**, 3-10 (2013).
 12. Nordgaard, J., Arnfred, S.M., Handest, P. & Parnas, J. The Diagnostic Status of First-Rank Symptoms. *Schizophrenia Bulletin* **34**, 137-154 (2008).
 13. Dickinson, D. et al. Attacking heterogeneity in schizophrenia by deriving clinical subgroups from widely available symptom data. *Schizophrenia bulletin* **44**, 101-113 (2018).
 14. Lim, K. et al. Cognitive subtyping in schizophrenia: a latent profile analysis. *Schizophrenia bulletin* **47**, 712-721 (2021).
 15. Arndt, S., Andreasen, N.C., Flaum, M., Miller, D. & Nopoulos, P. A longitudinal study of symptom dimensions in schizophrenia: prediction and patterns of change. *Archives of general psychiatry* **52**, 352-360 (1995).
 16. Chand, G.B. et al. Two distinct neuroanatomical subtypes of schizophrenia revealed using machine learning. *Brain* **143**, 1027-1038 (2020).
 17. Xiao, Y. et al. Subtyping Schizophrenia Patients Based on Patterns of Structural Brain Alterations. *Schizophrenia Bulletin* **48**, 241-250 (2021).
 18. Liang, S. et al. Aberrant triple-network connectivity patterns discriminate biotypes of first-episode medication-naïve schizophrenia in two large independent cohorts. *Neuropsychopharmacology* **46**, 1502-1509 (2021).
 19. Bak, N. et al. Two subgroups of antipsychotic-naïve, first-episode schizophrenia patients identified with a Gaussian mixture model on cognition and electrophysiology. *Translational psychiatry* **7**, e1087-e1087 (2017).
 20. Luo, C. et al. Subtypes of schizophrenia identified by multi-omic measures associated with dysregulated immune function. *Molecular Psychiatry* **26**, 6926-6936 (2021).
 21. Yin, L. et al. Leveraging genome-wide association and clinical data in revealing schizophrenia subgroups. *Journal of Psychiatric Research* **106**, 106-117 (2018).
 22. Gibson, G. Rare and common variants: twenty arguments. *Nature Reviews Genetics* **13**, 135-145 (2012).
 23. Owen, M.J. & Williams, N.M. Explaining the missing heritability of psychiatric disorders. *World Psychiatry* **20**, 294 (2021).
 24. Visscher, P.M., Yengo, L., Cox, N.J. & Wray, N.R. Discovery and implications of polygenicity of common diseases. *Science* **373**, 1468-1473 (2021).
 25. Lewis, C.M. & Vassos, E. Polygenic risk scores: from research tools to clinical instruments. *Genome Medicine* **12**, 44 (2020).
 26. Choi, S.W., Mak, T.S.-H. & O'Reilly, P.F. Tutorial: a guide to performing polygenic risk score analyses. *Nature*

- protocols* **15**, 2759-2772 (2020).
27. Climer, S., Templeton, A.R. & Zhang, W. Allele-specific network reveals combinatorial interaction that transcends small effects in psoriasis GWAS. *PLoS computational biology* **10**, e1003766 (2014).
 28. Wang, W. et al. Cassava genome from a wild ancestor to cultivated varieties. *Nature Communications* **5**, 5110 (2014).
 29. El-Moussaoui, M., Agouti, T., Tikniouine, A. & Adnani, M.E.L. A comprehensive literature review on community detection: Approaches and applications. *Procedia Computer Science* **151**, 295-302 (2019).
 30. Blondel, V.D., Guillaume, J.-L., Lambiotte, R. & Lefebvre, E. Fast unfolding of communities in large networks. *Journal of statistical mechanics: theory experiment* **2008**, P10008 (2008).
 31. Purcell, S. et al. PLINK: a tool set for whole-genome association and population-based linkage analyses. *The American journal of human genetics* **81**, 559-575 (2007).
 32. Flajnik, M.F. & Kasahara, M. Comparative Genomics of the MHC: Glimpses into the Evolution of the Adaptive Immune System. *Immunity* **15**, 351-362 (2001).
 33. Hargreaves, A. et al. The one and the many: effects of the cell adhesion molecule pathway on neuropsychological function in psychosis. *Psychological medicine* **44**, 2177-2187 (2014).
 34. Jia, P. et al. Network-assisted investigation of combined causal signals from genome-wide association studies in schizophrenia. *PLoS computational biology* **8**, e1002587 (2012).
 35. Borgatti, S.P. & Halgin, D.S. Analyzing affiliation networks. *The Sage handbook of social network analysis* **1**, 417-433 (2011).
 36. Barrat, A., Barthélemy, M., Pastor-Satorras, R. & Vespignani, A. The architecture of complex weighted networks. *Proceedings of the national academy of sciences* **101**, 3747-3752 (2004).
 37. Freeman, L. Centrality in networks: I. conceptual clarifications. social networks. *Social Network* (1979).
 38. Langville, A.N. & Meyer, C.D. A survey of eigenvector methods for web information retrieval. *SIAM review* **47**, 135-161 (2005).
 39. Page, L., Brin, S., Motwani, R. & Winograd, T. (Stanford InfoLab, 1999).
 40. Dogra, S. & Conn, P.J. Metabotropic glutamate receptors as emerging targets for the treatment of schizophrenia. *Molecular Pharmacology* **101**, 275-285 (2022).
 41. Zhang, Y. et al. Convergent lines of evidence support &NOTCH4& as a schizophrenia risk gene. *Journal of Medical Genetics* **58**, 666 (2021).
 42. Gao, X. et al. A study on the correlation between IL1RAPL1 and human cognitive ability. *Neuroscience letters* **438**, 163-167 (2008).
 43. Suvisaari, J., Keinänen, J., Eskelinen, S. & Mantere, O. Diabetes and Schizophrenia. *Curr Diab Rep* **16**, 16 (2016).
 44. Palmer, C.J. et al. Cdkal1, a type 2 diabetes susceptibility gene, regulates mitochondrial function in adipose tissue. *Mol Metab* **6**, 1212-1225 (2017).
 45. Bhat, S. et al. CACNA1C (Cav1. 2) in the pathophysiology of psychiatric disease. *Progress in neurobiology* **99**, 1-14 (2012).
 46. Weinberger, D.R. Thinking about schizophrenia in an era of genomic medicine. *American Journal of Psychiatry* **176**, 12-20 (2019).
 47. Climer, S., Templeton, A.R. & Zhang, W. Allele-specific network reveals combinatorial interaction that transcends small effects in psoriasis GWAS. *PLoS computational biology* **10**, e1003766 (2014).
 48. Mokhtari, R. & Lachman, H.M. The major histocompatibility complex (MHC) in schizophrenia: a review. *Journal of clinical cellular immunology* **7** (2016).
 49. Goddard, C.A., Butts, D.A. & Shatz, C.J. Regulation of CNS synapses by neuronal MHC class I. *Proceedings of the National Academy of Sciences* **104**, 6828-6833 (2007).
 50. Glynn, M.W. et al. MHCI negatively regulates synapse density during the establishment of cortical

- connections. *Nature neuroscience* **14**, 442-451 (2011).
51. Mei, L. & Xiong, W.-C. Neuregulin 1 in neural development, synaptic plasticity and schizophrenia. *Nature Reviews Neuroscience* **9**, 437-452 (2008).
 52. Forsyth, J.K. & Lewis, D.A. Mapping the Consequences of Impaired Synaptic Plasticity in Schizophrenia through Development: An Integrative Model for Diverse Clinical Features. *Trends Cogn Sci* **21**, 760-778 (2017).
 53. Nakazawa, K., Jeevakumar, V. & Nakao, K. Spatial and temporal boundaries of NMDA receptor hypofunction leading to schizophrenia. *npj Schizophrenia* **3**, 7 (2017).
 54. Forsyth, J.K. & Lewis, D.A. Mapping the consequences of impaired synaptic plasticity in schizophrenia through development: an integrative model for diverse clinical features. *Trends in cognitive sciences* **21**, 760-778 (2017).
 55. Chao-Gan, Y. & Yu-Feng, Z. DPARSF: A MATLAB Toolbox for "Pipeline" Data Analysis of Resting-State fMRI. *Frontiers in systems neuroscience* **4**, 13 (2010).
 56. Newman, M.E. Modularity and community structure in networks. *Proceedings of the national academy of sciences* **103**, 8577-8582 (2006).
 57. Abdi, H. & Williams, L.J. Principal component analysis. *Wiley interdisciplinary reviews: computational statistics* **2**, 433-459 (2010).
 58. Sculley, D. in Proceedings of the 19th international conference on World wide web 1177-1178 (2010).
 59. Watanabe, K., Taskesen, E., van Bochoven, A. & Posthuma, D. 17 - FUMA: FUNCTIONAL MAPPING AND ANNOTATION OF GENETIC ASSOCIATIONS. *European Neuropsychopharmacology* **29**, S789-S790 (2019).
 60. Consortium, G.O. The Gene Ontology (GO) database and informatics resource. *Nucleic acids research* **32**, D258-D261 (2004).
 61. Yan, C.-G., Wang, X.-D., Zuo, X.-N. & Zang, Y.-F.J.N. DPABI: data processing & analysis for (resting-state) brain imaging. **14**, 339-351 (2016).

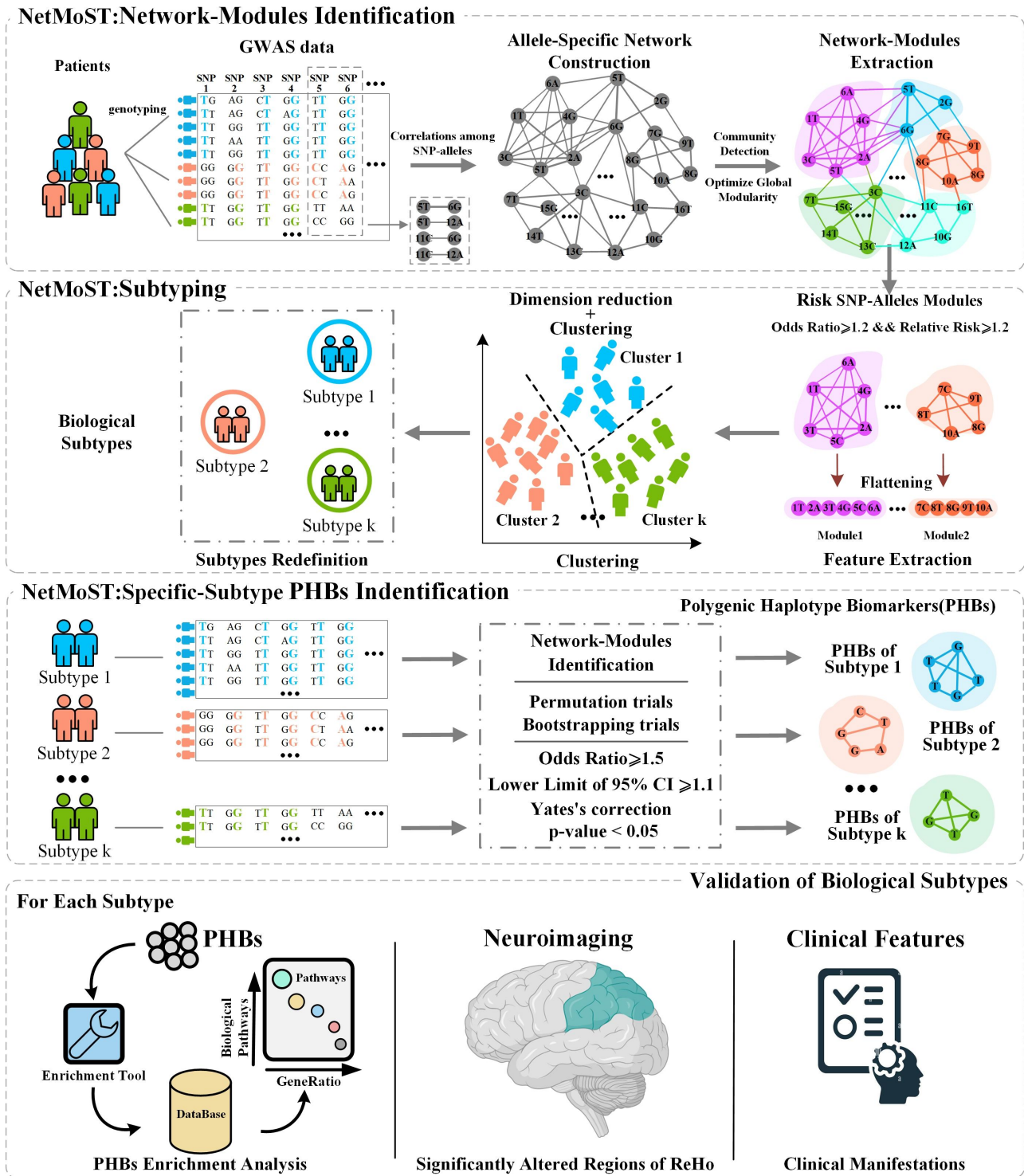


Figure 1 | Schematic of the NetMoST framework to define and validate objective subtypes of complex diseases. Stage one: Construction of specific SNP-allele network for complex diseases like SCZ and using Louvain community detection to extract risk SNP-alleles modules. Stage two: For the risk SNP-alleles modules of schizophrenia from stage one, the clustering method was applied to discover subtypes of schizophrenia. Stage three: The genetic variants of cases belonging to each subtypes were used to construct a new, subtype-specific SNP-allele network. Then the more stringent criteria ($OR \geq 1.5$, the lower limit of 95% $CI \geq 1.1$, and Yates's correction $p\text{-value} < 0.05$) to select subtype-specific PHBs that also underwent permutation and bootstrapping trials. Finally, the biological subtypes are validated utilizing multimodal data, including genetic profiles, brain neuroimaging, and clinical features. Firstly, the gene set enrichment analysis was applied to these PHBs for each

subtype to discover the unique genetic pattern. Furthermore, the neuroimaging and clinical features were examined to determine other biological distinctions within the alleles-module-based subtypes.

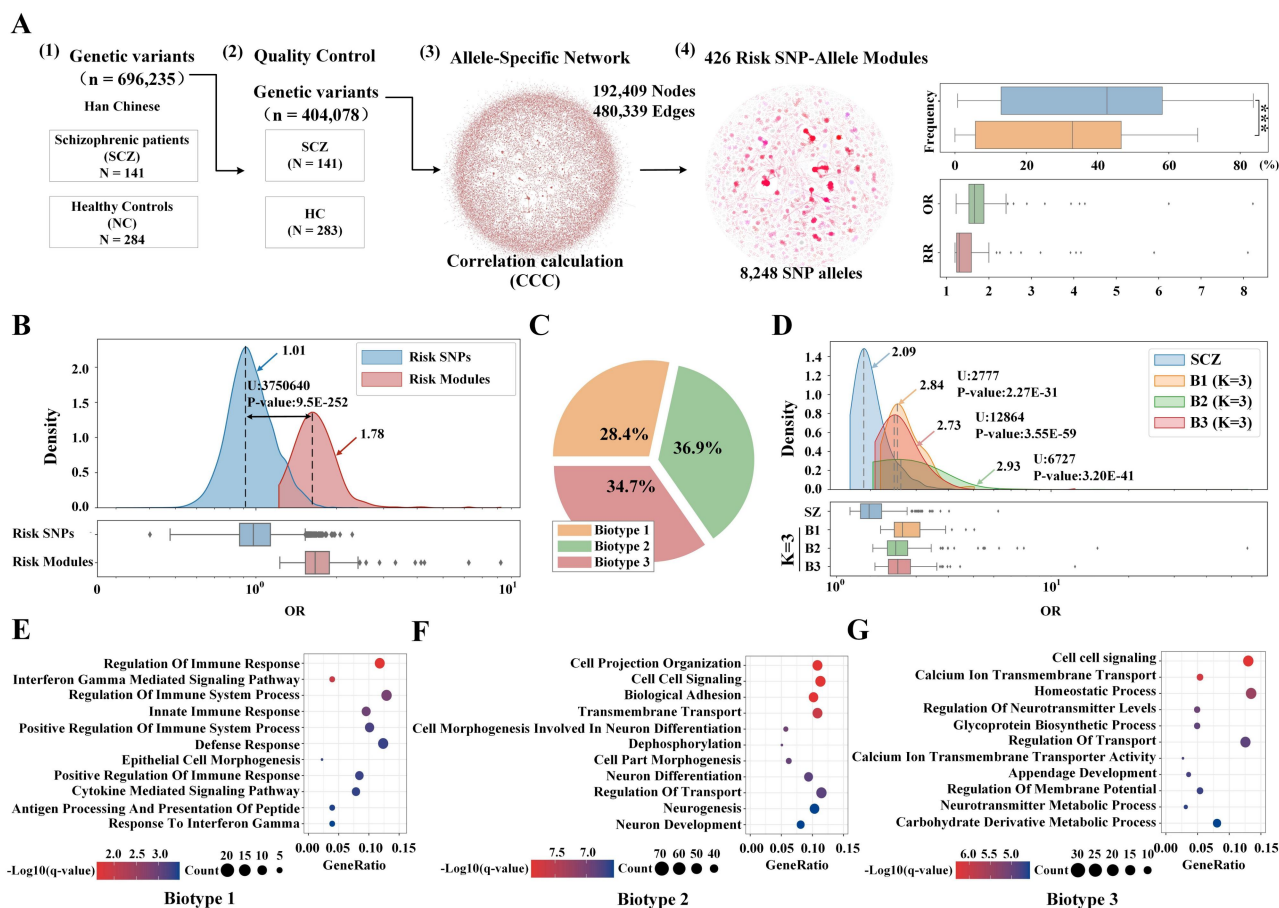


Figure 2 | NetMoST method was applied to subtype schizophrenia (SCZ) and define three biological subtypes of SCZ based on risk SNP-alleles modules. A) standard quality control procedures were carried out on the genetic variations dataset. Finally, 404,078 SNPs were retained, and 141 and 283 subjects were labeled as schizophrenic cases and healthy controls, respectively. Based on these SNP alleles that passed quality control, a specific SNP-allele network with 192,409 nodes (SNP-alleles) and 480,339 edges (associations of SNP-allele pairs) was established for SCZ, and 426 risk SNP-alleles modules ($OR \geq 1.2$ and $RR \geq 1.2$) highly associated with SCZ were identified. **B)** These single SNPs within the risk modules had lower OR values than the OR of risk SNP-allele modules, which indicates the necessity of capturing combinatorial genetic risk for complex disease. **C)** The quantitative distribution of three biotypes for SCZ subjects. The netMoST framework identified three biological subtypes, with biotypes 1, 2, and 3 have 40, 52, and 49, respectively. **D)** The odds ratios of PHBs of each subtype after subtyping were significantly higher than before subtyping. This further explained that accurate classification would improve the power to recognize polygenic signatures. **E-G)** Significant biological characteristics across three biotypes of SCZ. Examining biological characteristics from genomics between each biotype and HC revealed the three biotypes had unique genetic patterns. Gene set enrichment of PHBs for each biotype. PHBs highly associated with biotype 1 are significantly enriched in the process of related-immune function, biotype 2 involved in nervous system development, including neuron development and differentiation, as well as neurogenesis, and biotype 3 has more emphasis on the transport of calcium ions and neurotransmitters.

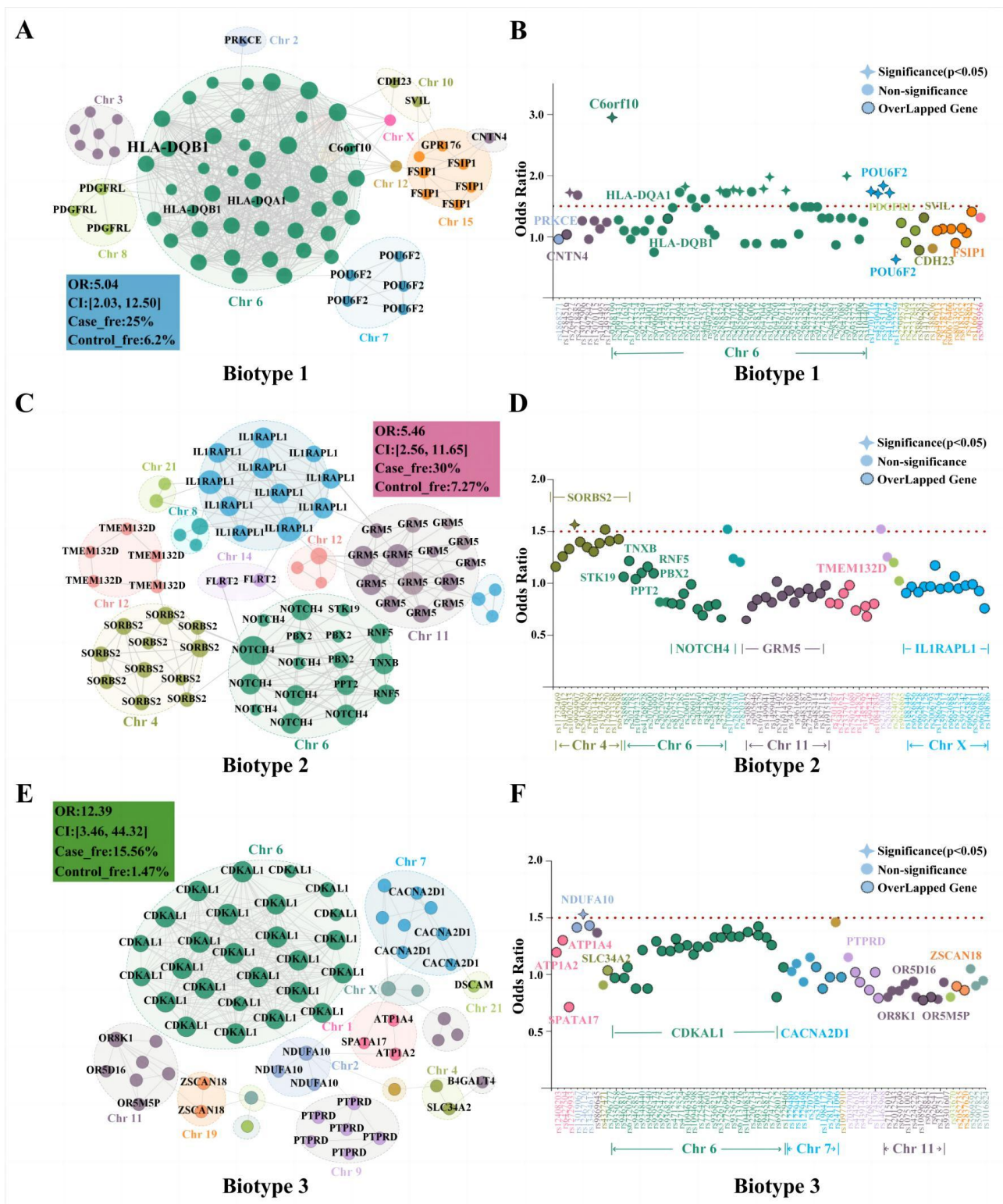


Figure 3 | The subtype-specific polygenic haplotype biomarker capable of exhibiting unique genetic characteristics for each biotype of SCZ. The novel netMoST method was introduced to discover genetic subtypes based on SNP-alleles modules and identified three biotypes of SCZ. The subtype-specific representative PHB with higher OR capable of exhibiting unique genetic characteristics for each biotype was extracted through the construction of specific SNP-alleles networks and community detection. **A-C)** Topological network structure for SNP alleles (Each node label was named by its overlapping gene) of subtype-specific PHB with higher OR for each biotype. Each SNP allele is represented by a node, where its size is proportional to the node degree in this network, and its color represents its chromosome. **D-F)** The odds ratio of each SNP of the subtype-specific PHBs with higher OR of each biotype. The horizontal axis represents the SNP for SPHB of each subtype, and the

vertical axis represents the odds ratio of SNP. Each SNP is represented by a node whose color represents its chromosome. The three representative PHBs reveal that netMoST could identify combinatorial genetic risk factors easily neglected by conventional single-marker-based methods due to the smaller OR. These genetic risk factors may significantly form large haplotypes with long-range linkage associations by spanning multiple chromosomes.

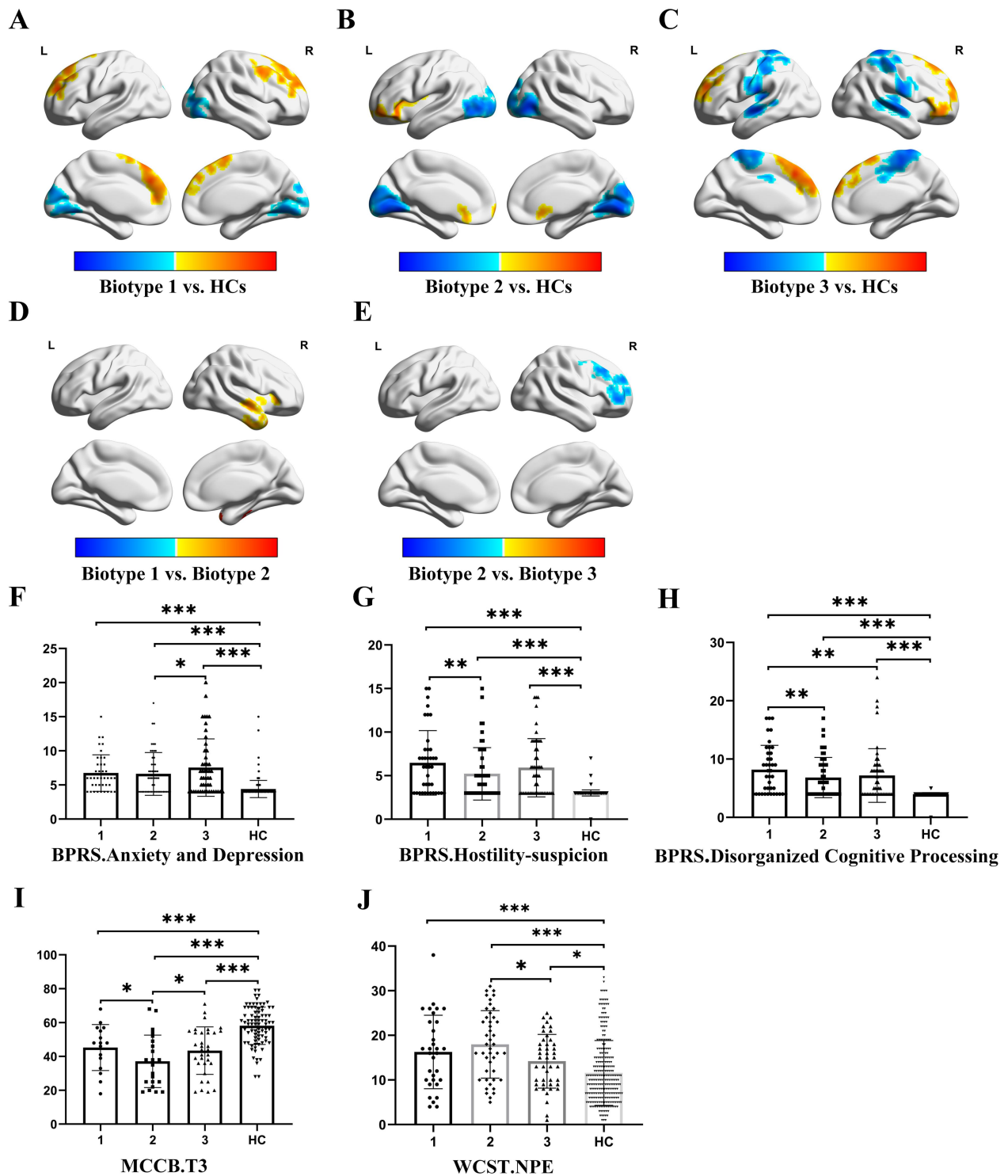


Figure 4 | Significant differences in brain neuroimaging and clinical characteristics among three biotypes of SCZ. A-C) The neuroimaging regional homogeneity (ReHo) alterations between each biotype and HCs. D-E) The neuroimaging regional homogeneity (ReHo) alterations among three biotypes. F-H) The differences in behavioral symptoms assessed by the Brief Psychiatric Rating Scale (BPRS) among three biotypes and HCs. I-J) The cognitive ability between three biotypes of SCZ. Biotype 2 performed worse on cognitive measures than the other two biotypes due to the lower score of T3 and the greater score of NPE belonging to the MATRICS Consensus Cognitive Battery (MCCB) and the Wisconsin Card Sorting Test (WCST), respectively. The vertical black lines show the standard errors of the means, and the significance level was set to $p < 0.05$ with the least significant difference correction. *** $p < 0.001$; ** $p < 0.01$; * $p < 0.05$.